Cotransport of viruses and clay particles in water saturated and unsaturated porous media

Vasiliki I. Syngouna [1] and Constantinos V. Chrysikopoulos [2]

[1] Environmental Engineering Laboratory, Civil Engineering Department, University of Patras, Patras 26500, Greece (kikisygouna@upatras.gr)

[2] School of Environmental Engineering, Technical University of Crete, Chania 73100, Greece (cvc@enveng.tuc.gr)

AGU American Geophysical Union

2014 Fall Meeting: H31C-0626

Biomet BioNFate

Πανεπιστήμιο Πατρών University of Patras

Technical University of Crete

Abstract

This experimental study examines the effects of clay colloids on the transport of viruses in variably saturated porous media. The experimental data indicated that the mass recovery of viruses and clay colloids decreased as the water saturation decreased. The various experimental collision efficiencies were determined using the classical colloid filtration theory. Temporal moments of the various breakthrough concentrations collected, suggested that the presence of clays significantly influenced virus transport and irreversible deposition onto glass beads. The mass recovery of both viruses, based on total effluent virus concentrations, was shown to reduce in the presence of suspended clay particles. Furthermore, the transport of suspended virus and clay-virus particles was retarded, compared to the conservative tracer. Under unsaturated conditions both clay particles facilitated the transport of ΦX174 while hindered the transport of MS2. Moreover, the surface properties of viruses, clays and glass beads were employed for the construction of classical DLVO and capillary potential energy profiles, and the results suggested that capillary forces play a significant role on colloid retention. It was estimated that the capillary potential energy of MS2 is lower than that of ΦX174, and the capillary potential energy of KGa-1b is lower than that of STx-1b, assuming that the protrusion distance through the water film is the same for each pair of particles. Moreover, the capillary potential energy is several orders of magnitude greater than the DLVO energy potential.

Materials and methods

Bacteriophages

MS2: an F-specific single-stranded RNA phage with effective particle diameter ranging from 24 to 26 nm

ΦX174: a somatic single-stranded DNA phage with effective particle diameter ranging from 25 to 27 nm

For the separation of viruses adsorbed onto clay particles from suspended viruses in the liquid phase, centrifugation was used as described in Syngouna and Chrysikopoulos (2013).

Clays

Kaolinite (KGa-1b): a well-crystallized kaolin from Washington County, Georgia

Montmorillonite (STx-1b): a Ca-rich montmorillonite, white, from Gonzales County, Texas

The <2 μm clay colloidal fraction was separated by sedimentation and then was purified (Rong et al., 2008)

Experimental Set Up

- Plexiglass column
  - Length 15.2 cm
  - Internal diameter 2.6 cm
- Uniformly wet-packed
- Glass beads 2mm
- Flow rate of Q=1.5 mL/min
- pH 7.0±0.2
- Saturation level: 81-100%
- Water potential: constant

(a) Saturated cotransport

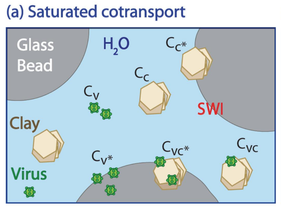

(b) Unsaturated cotransport

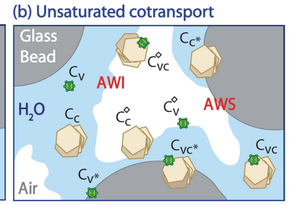

AWI: air-water interface
AWS: air-water-solid
SWI: solid-water interface

Colloid filtration theory

Experimental attachment efficiency (Kretzschmar et al., 1999):

$$\alpha_{exp} = -\frac{2}{3}\frac{d_c}{L(1-\theta_m)\eta_0}\ln\left[\frac{C_{ss}}{C_0}\right]$$

where:

- θ_m [-] is the moisture content
- d_c [L] is the mean collector diameter
- C_0 [M/L^3] is the influent colloid concentration
- C_{ss} [M/L^3] is the effluent colloid concentration (steady state conditions)
- η_0 is the single-collector contact efficiency (Tufenkjii and Elimelech, 2004)

Capillary energy calculations

Total vertical capillary force $F_{v\text{-}tot}$ (Gao et al., 2008):

$$F_{v\text{-}tot} = \sigma_{aw} 2\pi\sqrt{r_p^2 - (h_f - r_p)^2}\cos\left[\beta + \frac{\pi}{2} - \cos^{-1}\left(\frac{h_f - r_p}{r_p}\right)\right]$$

Capillary potential energy, Φ_c (Gao et al., 2008):

$$\Phi_c = \int_{z=r_p(1-\cos\beta)}^{z=d_f} F_{v\text{-}tot}\,dz$$

$$= \int_{z=r_p(1-\cos\beta)}^{z=d_f} \sigma_{aw} 2\pi\sqrt{r_p^2 - (r_p - z)^2}\cos\left[\beta + \frac{\pi}{2} - \cos^{-1}\left(\frac{r_p - z}{r_p}\right)\right]dz$$

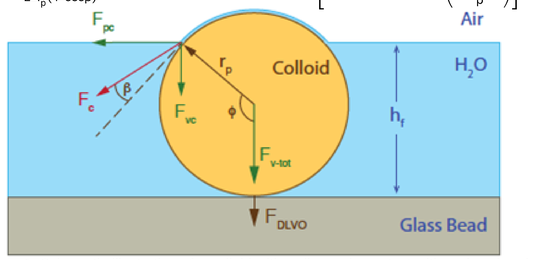

Figure 1. Schematic illustration of a colloid with radius r_p, in contact with a glass bead, trapped in a thin water film with thickness h_f.

Results and discussion

Transport experiments

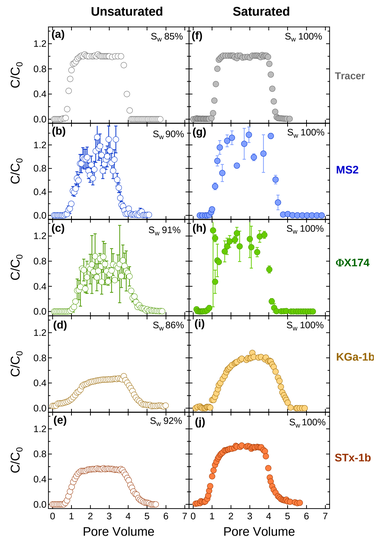

Figure 2. Breakthrough data from the transport experiments with tracer, viruses (MS2, ΦX174), and clays (KGa-1b, STx-1b) in unsaturated (a-e: open symbols), and saturated (f-j: filled symbols) columns packed with glass beads.

Cotransport experiments $C_{Total\text{-}v} = C_v + C_{vc}$

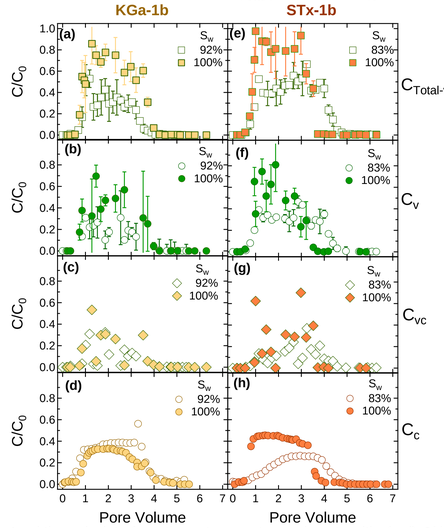

Figure 3. Breakthrough data from the cotransport experiments with: (a-d) ΦX174-KGa-1b, and (e-h) ΦX174-STx-1b in saturated (filled symbols), and unsaturated (open symbols) columns packed with glass beads. The concentrations $C_{Total\text{-}v}$ are presented in (a,e), C_v in (b,f), C_{vc} in (c,g), and C_c in (d,h).

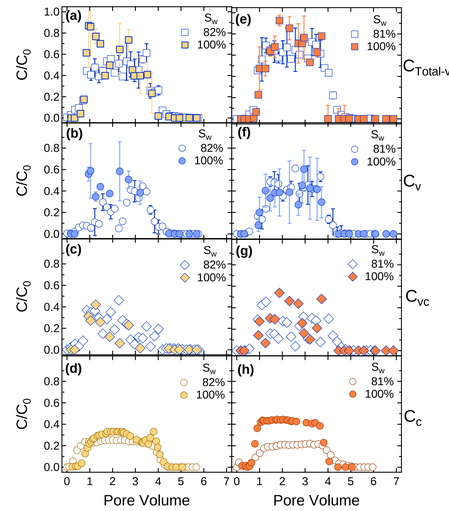

Figure 4. Breakthrough data from the cotransport experiments with: (a-d) MS2-KGa-1b, and (e-h) MS2-STx-1b in saturated (filled symbols), and unsaturated (open symbols) columns packed with glass beads. The concentrations $C_{Total\text{-}v}$ are presented in (a,e), C_v in (b,f), C_{vc} in (c,g), and C_c in (d,h).

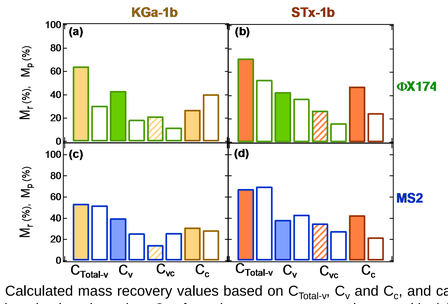

Figure 5. Calculated mass recovery values based on $C_{Total\text{-}v}$, C_v and C_c, and calculated mass produced values based on C_{vc}, from the cotransport experiments with: (a) ΦX174 and KGa-1b, (b) ΦX174 and STx-1b, (c) MS2 and KGa-1b, and (d) MS2 and STx-1b under saturated (filled columns) and unsaturated (open columns) conditions.

Table 1. Experimental conditions and estimated parameters for the cotransport experiments

Experiment	Initial Concentration	θ (–)	θ_m (–)	S_w (–)	U (cm/min)	M_r (%) for $C_{Total\text{-}v}$ or C_c	M_r (%) for C_v	M_p (%) for C_{vc}	M_{10}/M_{00} for $C_{Total\text{-}v}$ or C_c	M_{10}/M_{00} for C_v	M_{10}/M_{00} for C_{vc}	$\alpha_{Total\text{-}v}$ (–)	α_v (–)
Transport Experiments													
Tracer	0.01 mol/L	0.42	–	1.00	0.74	100.0	–	–	1.00	–	–	–	–
Tracer	0.01 mol/L	0.41	0.38	0.93	0.66	111.0	–	–	1.00	–	–	–	–
ΦX174	3817 PFU/mL	0.42	–	1.00	0.74	100.0	–	–	0.90	–	–	0.00	–
ΦX174	3450 PFU/mL	0.41	0.38	0.91	0.66	64.9	–	–	1.31	–	–	0.13	–
MS2	4842 PFU/mL	0.42	–	1.00	0.74	100	–	–	1.00	–	–	0.00	–
MS2	13150 PFU/mL	0.42	0.38	0.90	0.58	76.6	–	–	1.26	–	–	0.08	–
KGa-1b	67.6 mg/L	0.42	–	1.00	0.74	79.5	–	–	1.10	–	–	0.15	–
KGa-1b	69.28 mg/L	0.40	0.38	0.86	0.70	49.3	–	–	1.23	–	–	0.70	–
STx-1b	102.3 mg/L	0.42	–	1.00	0.74	93.8	–	–	1.00	–	–	0.03	–
STx-1b	88.06 mg/L	0.41	0.38	0.92	0.69	59.1	–	–	1.26	–	–	0.35	–
Cotransport Experiments													
ΦX174–KGa-1b	(2767 PFU/mL)–(80.8 mg/L)	0.42	–	1.00	0.74	(64.6) –(27.2)	43.4	21.6	(0.82)–(0.87)	0.83	0.79	(0.08) –(0.86)	0.15
ΦX174–KGa-1b	(5100 PFU/mL)–(75.0 mg/L)	0.42	0.39	0.92	0.64	(30.6) –(40.6)	18.7	12.0	(1.01)–(1.13)	1.01	1.02	(0.18) –(1.00)	0.37
ΦX174–STx-1b	(4817 PFU/mL)–(122.2 mg/L)	0.42	–	1.00	0.74	(71.9) –(47.7)	43.0	27.2	(0.79)–(0.77)	0.82	1.01	(0.06) –(0.29)	0.15
ΦX174–STx-1b	(7433 PFU/mL)–(107.0 mg/L)	0.45	0.37	0.83	0.72	(53.5) –(25.1)	37.3	16.2	(1.11)–(1.18)	1.08	1.18	(0.18) –(0.83)	0.29
MS2–KGa-1b	(9767 PFU/mL)–(77.0mg/L)	0.42	–	1.00	0.74	(53.8) –(31.4)	40.0	14.7	(0.78)–(0.85)	0.85	0.70	(0.11) –(0.77)	0.16
MS2–KGa-1b	(21383 PFU/mL)–(69.0 mg/L)	0.43	0.37	0.83	0.72	(52.2) –(28.6)	25.8	26.0	(1.08)–(1.01)	1.20	0.96	(0.17) –(1.00)	0.36
MS2–STx-1b	(9500 PFU/mL)–(92.6 mg/L)	0.42	–	1.00	0.74	(67.7) –(42.9)	38.5	35.1	(0.89)–(0.85)	0.92	0.93	(0.07) –(0.33)	0.17
MS2–STx-1b	(11067 PFU/mL)–(89.0 mg/L)	0.43	0.35	0.81	0.70	(70.0) –(22.0)	43.4	27.9	(1.09)–(1.12)	1.00	1.06	(0.09) –(0.85)	0.21

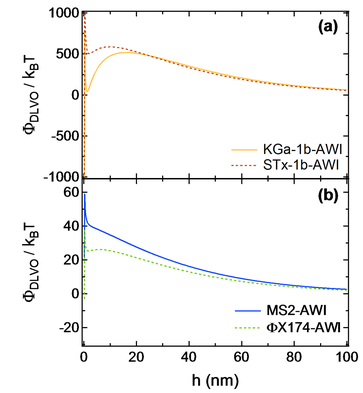

Figure 6. Predicted DLVO energy interactions as a function of separation distance, based on the sphere-plate model for: (a) KGa-1b-AWI, STx-1b-AWI, and (b) MS2-AWI, ΦX174-AWI.

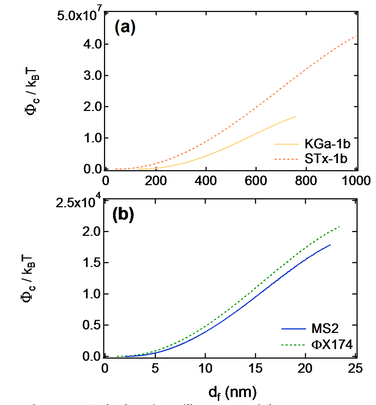

Figure 7. Calculated capillary potential energy Φ_c as a function of d_f for: (a) clay colloids (KGa-1b, STx-1b), and (b) viruses (MS2, ΦX174) retained within thin water films and at AWmS interfaces.

Conclusions

- The mass recovery of viruses and clay colloids decreased as the water saturation decreased.
- The mass recovery of both viruses was shown to reduce in the presence of suspended clay particles.
- Under saturated conditions, the transport of both $C_{Total\text{-}v}$ and C_v was retarded, compared to the conservative tracer while under unsaturated conditions the opposite was observed.
- Under unsaturated conditions both clay particles facilitated the transport of ΦX174 while hindered the transport of MS2.
- In the presence of STx-1b, the C_{vc}=$C_{Total\text{-}v}$-C_v values of both viruses were higher than those in the presence of KGa-1b under both saturated and unsaturated conditions.
- In the presence of both KGa-1b and STx-1b, $\alpha_{Total\text{-}v}$ and α_v values increased with decreasing saturation level.
- The capillary potential energy of MS2 is lower than that of ΦX174, and the capillary potential energy of KGa-1b is lower than that of STx-1b, assuming that the protrusion distance through the water film is the same for each pair of particles.
- The capillary potential energy is several orders of magnitude greater than the DLVO potential energy.

References

V.I. Syngouna, C.V. Chrysikopoulos, *Colloids Surf. A: Physicochem. Eng. Aspects* 416 (2013) 56-65.

X. Rong, Q. Huanga, X. He, H. Chen, P. Cai, W. Liang, *Colloids Surf. B: Biointerfaces* 64 (2008) 49–55.

R. Kretzschmar, M. Borkovec, D. Grolimund, M. Elimelech, *Adv. Agron*. 65 (1999) 121–193.

N. Tufenkji, M. Elimelech, *Environ. Sci. Technol*. 38 (2004) 529–536.

B. Gao, T. S. Steenhuis, Y. Zevi, V. L. Morales, J. L. Nieber, B. K. Richards, J. F. McCarthy, and J.-Y. Parlange, *Water Resour. Res.*, 44 (2008) W04504, doi:10.1029/2006WR005332.

This research has been co-financed by the European Union (European Social Fund-ESF) and Greek national funds through the Operational program "Education and Lifelong Learning" of the National Strategic Reference Framework (NSRF)-Research Funding Programs: Heracleitus II and Aristeia I (No. 1185). Investing in knowledge society through the European Social Fund.